ADVANCED
PHOTONICS
RESEARCH
Open Access
www.adpr-journal.com

An Efficient Aggregation-Induced Emission Supramolecular Probe for Detection of Nitroaromatic Explosives in Water

*Xuan Zhao, Yong Chen, XianYin Dai, WeiLei Zhou, JingJing Li, and Yu Liu**

Nitroaromatic compounds (NACs) are the components of explosives that pose a serious hazard to the environment and human health, especially 2,4,6-trinitrophenol (TNP), which has strong explosibility and good water solubility. An effective supramolecular fluorescent probe for nitroaromatic detection is prepared based on the sulfato-β-cyclodextrin (SCD)-induced molecular aggregation of 9,10-bis{4-[2-(*N*,*N*,*N*-trimethylammonium)hexyloxy]styrene} anthracene dibromide (AnEA) and subsequent aggregation-induced emission, which presents high sensitivity particularly toward TNP with a detection limit of 586 ppb in water and 23 ppb on the test paper. Herein, a convenient and effective supramolecular means for nitro-detection in water is provided.

1. Introduction

Nitroaromatic (NAC) explosives in water have been listed as "priority pollutants" by the United Stated Environmental Protection Agency because of their serious environmental and human health hazards.[1,2] In particular, 2,4,6-trinitrophenol (TNP) has high explosion power and is commonly used in industries such as explosives, pharmaceuticals, leathers, and dyes.[3–6] TNP can easily cause pollution in the soil and groundwater once released into the environment and is difficult to degrade due to electron deficiency.[7–9] In addition, TNP has severe irritation and biotoxicity, thus causing hazardous effects on human health such as anemia, headache, liver malfunctioning, and carcinogenicity,[10–12] because it can be metabolized into picramic acid, which is ten times more mutagenic than TNP when reaching the digestive cycle of mammalians.[13,14] Therefore, it is of great significance to develop a simple, rapid, and sensitive method for the detection of nitroaromatic compounds (NACs).

Currently, although various methods have been applied for the determination of NACs including ion mobility spectrometry,[15–17] electrochemical assay,[18,19] mass spectrometry,[20,21] surface-enhanced Raman spectroscopy,[22,23] fluorescence probes,[24,25] etc. Most of these have disadvantages of complicated operations, sample pretreatments, and high costs. Among them, fluorescence probes, such as nanofibers,[26,27] gels,[28–30] graphene quantum dots,[31] small-molecule sensors,[32] fluorescent organic nanoparticles (FONs),[33] metal-organic frameworks,[34,35] and supramolecular polymers,[36,37] provide effective solutions in the field of NAC detection due to high sensitivity, short response time, convenience, and low cost (Table S1, Supporting Information). Huang and coworkers constructed a supramolecular polymer network by a TPE-containing conjugated polymer with pendent pillararene units (P5-TPE) and a symmetric BB type crosslinker (G),[38] and the fluorescence intensity of the supramolecular polymer network decreased after adding nitro-compound explosives. Liu and coworkers synthesized a superbenzene-bridged bis-(permethyl-β-cyclodextrin) by attaching two permethyl β-cyclodextrin (β-CD) units onto a coronene core, showing the specific fluorescence responses to nitroaromatic explosives.[39] Although the rigid π-conjugated supramolecular polymers show good sensitivity toward NACs through the optical signal amplification effect compared with small-molecule sensors, they still suffer from complex synthesis, long-time consumption, low solubility, and yield. It is also noteworthy that most of the detection processes in previous reports were realized in organic media or organic–water mixture media, which greatly limited the practical application of these sensors for the NAC detection in water. Therefore, it is very important to develop a simple approach to prepare fluorescent probes with easy operation, high solubility, and sensitivity to detect NACs at low concentrations in water.

Herein, a water-soluble supramolecular assembly (SCD–AnEA) was synthesized based on the sulfato-β-cyclodextrin (SCD)–induced molecular aggregation of 9,10-bis{4-[2-(*N*,*N*,*N*-trimethyl ammonium)hexyloxy]styrene} anthracene dibromide (AnEA) through host–guest noncovalent interactions (**Scheme 1**). There are many advantages of this system: 1) 9,10-distyrylanthrance derivatives have good electron-donating properties and can enhance the fluorescence emission in the aggregated state due to the aggregation-induced emission (AIE) effect.[40,41] 2) SCD, a kind of sulfonate-modified cyclic oligosaccharide, is

X. Zhao, Prof. Y. Chen, Dr. X. Dai, Dr. W. Zhou, J. Li, Prof. Y. Liu
College of Chemistry
State Key Laboratory of Elemento-Organic Chemistry
Nankai University
Tianjin 300071, P. R. China
E-mail: yuliu@nankai.edu.cn

Prof. Y. Liu
Collaborative Innovation Center of Chemical Science and Engineering
Tianjin 300071, China

The ORCID identification number(s) for the author(s) of this article can be found under https://doi.org/10.1002/adpr.202000007.

DOI: 10.1002/adpr.202000007

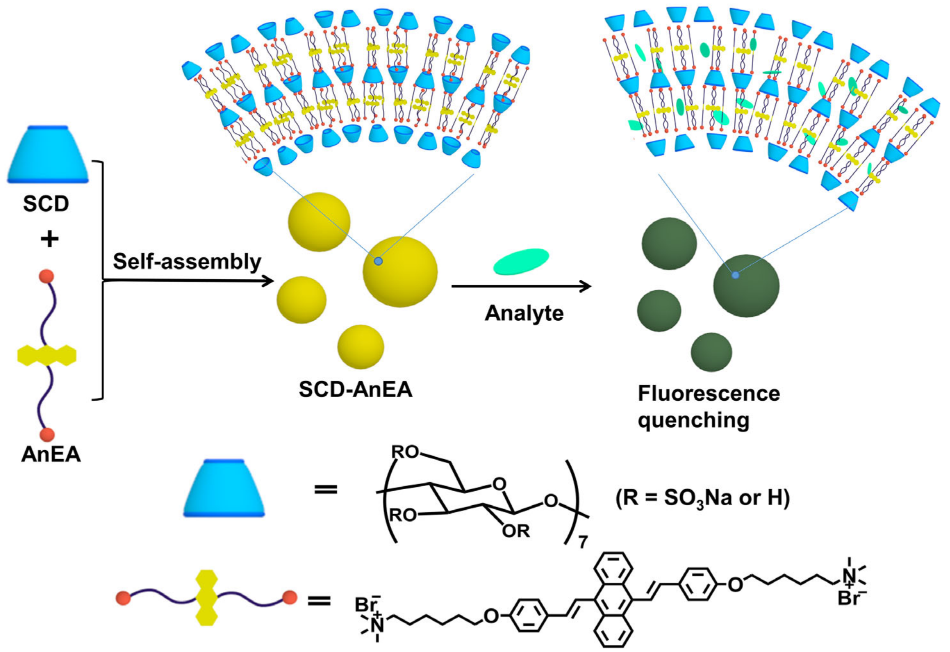

Scheme 1. Schematic illustration of SCD–AnEA supramolecular assembly.

of excellent water solubility, nontoxicity, and environmental friendliness, and more importantly, SCD with high negative charge density can form supramolecular assembly with the cationic AnEA in water.[42] 3) This supramolecular assembly is simple to prepare and exhibits not only the good photoluminescence property but also the high detection universality to NACs at a low concentration as well as the ppb-level detection limit to TNP. This work provides an applicable and novel supramolecular strategy for the construction of fluorescent probes for nitroaromatic explosives in water, which greatly expands its application in the field of pollutant detection.

2. Results and Discussion

2.1. Construction of SCD–AnEA Supramolecular Probe

The solvent-dependent aggregation behavior of AnEA was investigated by fluorescence spectroscopy. Fluorescence intensities of AnEA in organic solvents were very weak, indicating that no self-aggregation of AnEA occurred (Figure S4, Supporting Information). In water/acetonitrile mixtures, the fluorescence intensity of AnEA obviously enhanced with an increasing volume fraction of water (Figure S5, Supporting Information) due to the AIE property, which is consistent with the previous reports.[40,41,43] Interestingly, AnEA showed distinct yellow fluorescence emission with the addition of SCD in aqueous solution when excited at 420 nm (Figure S6, Supporting Information). A possible reason may be that SCD induced the aggregation of AnEA in water, leading to the AIE emission. Therefore, the induced aggregation behavior of SCD toward AnEA was investigated by optical transmittance, Tyndall effect, quantum yield, and fluorescence lifetime measurements. By monitoring the dependence of the optical transmittance of AnEA at 600 nm, the critical aggregation concentrations (CAC) values of AnEA with and without SCD were measured.[44] As shown in **Figure 1**a,c, the optical transmittance of the free AnEA at 600 nm was nearly unchanged with concentrations increasing from 5×10^{-7} to 9×10^{-5} M, indicating that free AnEA could not self-aggregate in this concentration range. However, the optical transmittance of AnEA at 600 nm greatly decreased in the presence of SCD within the same concentration range, and an inflection point at 2.78×10^{-5} M was observed on the plot of optical transmittance versus concentration (Figure 1b,d), indicating that SCD could greatly decrease the CAC value of AnEA. Moreover, the preferable mixing ratio between SCD and AnEA was also determined by gradually adding SCD to an AnEA solution at a fixed concentration of 4×10^{-5} M. The optical transmittance of AnEA at 525 nm decreased rapidly and then gradually increased with the addition of SCD, and the minimum was reached when the SCD/AnEA ratio was 1:7 (Figure S7, Supporting Information). In addition, the fluorescence lifetimes of AnEA were measured as $\tau_1 = 0.98$ ns and $\tau_2 = 4.35$ ns (Figure S8 and Table S1, Supporting Information), but these values increased to $\tau_1 = 2.07$ ns and $\tau_2 = 6.08$ ns after the addition of SCD. In contrast, the quantum yield of the SCD–AnEA system was measured as 11.45%, which was 6.1 times higher than that of free AnEA (1.89%, Figure S9, Supporting Information). Furthermore, a simple mixture of SCD with AnEA in water showed a strong Tyndall effect, but either the free AnEA or SCD alone did not exhibit any Tyndall effect under the comparable condition (Figure S10, Supporting Information). These phenomena jointly demonstrated the formation of a large aggregate between SCD and AnEA.

Dynamic light scattering (DLS), scanning electron microscopy (SEM), and transmission electron microscopy (TEM) gave information on the morphology of the SCD–AnEA aggregate.

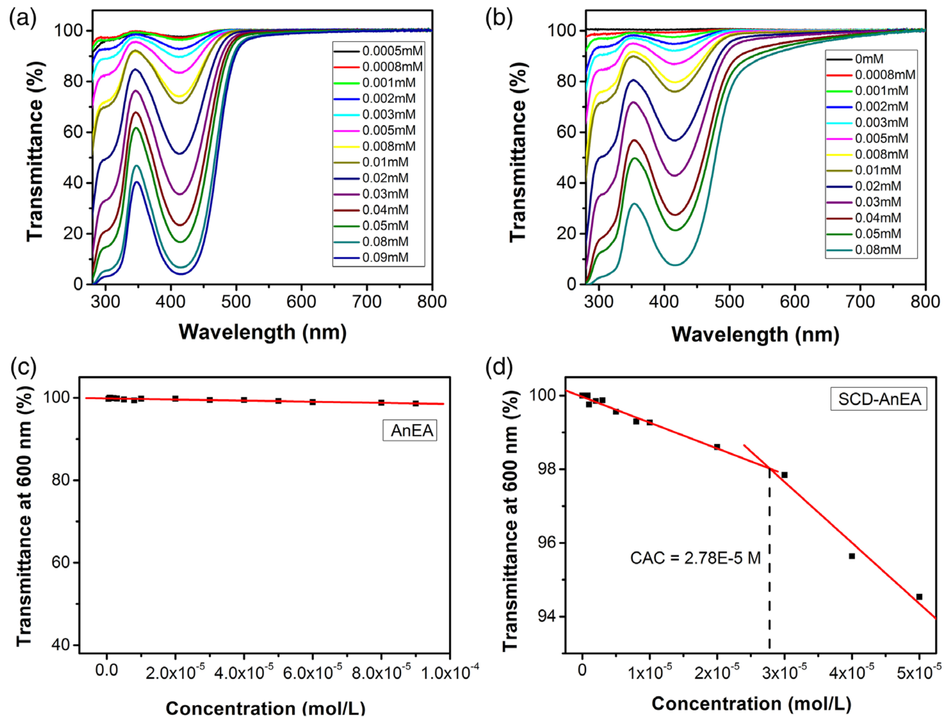

Figure 1. Optical transmittance of aqueous solutions of AnEA at different concentrations: a) without and b) with SCD (1×10^{-4} M) at 25 °C. Dependence of the optical transmittance at 600 nm on AnEA concentration c) without and d) with SCD (1×10^{-4} M).

The SEM and TEM images of the SCD–AnEA aggregate showed a number of nanoparticles with diameters ranging from 50 to 100 nm (Figure S11, Supporting Information), which were a little smaller than the hydrodynamic diameter (138.3 nm) measured by DLS measurement (**Figure 2**a and Figure S12, Supporting Information). Moreover, the zeta potential of the SCD–AnEA aggregate was measured as −8.85 mV (Figure 2b), suggesting that the surface of the nanoparticle was mainly covered by excellent water solubility and anionic SCD. Accordingly, the possible assembly mechanism of SCD–AnEA is shown in Scheme 1. Herein, one anionic SCD and several cationic AnEA molecules were induced to form a complex in water mainly via the electrostatic interactions and then convolved and aggregated to nanoparticles, the surface of which was covered by some negative charges. This aggregation structure greatly weakened the intermolecular and intramolecular rotation of AnEA. Thus, the excited AnEA molecules could mainly return to the ground state via the radiative transition, leading to the intense fluorescent emission.[45,46]

2.2. Detection of NACs in Water

Subsequently, the versatility and selectivity of the SCD–AnEA assembly for the detection of NACs were investigated by fluorescence spectroscopy with various nitroaromatic explosives as model substrates (Figure S13, Supporting Information). **Figure 3** shows the fluorescence quenching efficiency of SCD–AnEA assembly at 525 nm for different NACs. In the control experiments, the free AnEA gave the fairly weaker detection ability to NACs than SCD–AnEA because the fluorescence

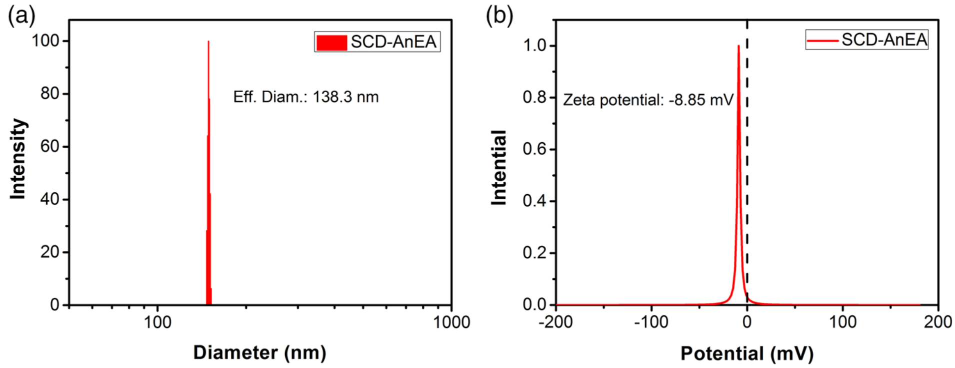

Figure 2. a) DLS data and b) zeta potential of SCD–AnEA assembly (5.71×10^{-6} M 4×10^{-5} M) in water at 25 °C.

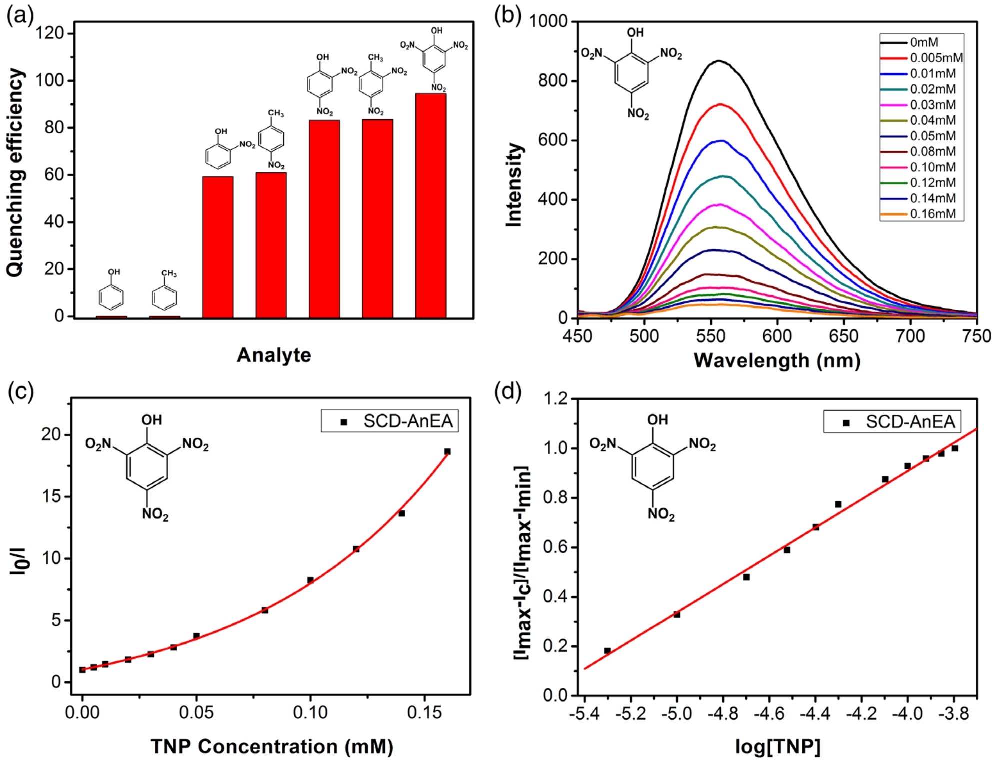

Figure 3. a) Quenching efficiency of SCD–AnEA in water toward various exploders; b) Emission spectra of SCD–AnEA in water toward TNP at various concentrations ($\lambda_{ex} = 420$ nm); c) SV plot for quenching of SCD–AnEA with TNP in water; d) $(I_{max}–I)/(I_{max}–I_{min})$ versus log[TNP] plots for SCD–AnEA in water.

intensity of free AnEA was 5.5 times lower than that of SCD–AnEA at a low concentration (4×10^{-5} M) in aqueous solution. In a typical comparison, the fluorescence quenching value of SCD–AnEA (5.71×10^{-6} M/4×10^{-5} M) was 6.6 times higher than that of the free AnEA (4×10^{-5} M) toward TNP (Figure S14, Supporting Information). Interestingly, different degrees of fluorescence quenching were observed with the addition of various nitroaromatics to the SCD–AnEA aqueous solution, but the fluorescence of SCD–AnEA was nearly unchanged with the addition of nitrogen-free aromatic compounds such as toluene and phenol ($0–1.6 \times 10^{-4}$ M). As shown in Figure 3, the fluorescence of SCD–AnEA gradually quenched with the gradual addition of trinitrophenol (TNP), and the quenching efficiency ($(I_0–I)/I_0 \times 100\%$) could reach 95% with a concentration of TNP as 1.6×10^{-4} M. In addition, the bright yellow fluorescence of SCD–AnEA turned colorless with the addition of TNP, which could be clearly observed by the naked eye (Figure S15, Supporting Information). Similarly, the quenching efficiencies of SCD–AnEA for other substrates were measured as ≈60% for *o*-nitrophenol (ONP) and *p*-nitrotoluene (PNT) and ≈80% for dinitrophenol (DNP) and dinitrotoluene (DNT), respectively. These phenomena jointly indicated the efficient detection ability of SCD–AnEA probe toward nitroaromatics. The fluorescence quenching degree of SCD–AnEA increased with the increase in the number of nitro-groups on NACs, and the most electron-deficient molecule TNP showed the largest fluorescence quenching. In the control experiment, the absorbance intensity of NACs was almost unchanged with the addition of SCD (Figure S16, Supporting Information), indicating that no inclusion complexation occurred between SCD and free NAC. Moreover, the fluorescence intensity of the SCD–AnEA assembly was significantly reduced when TNP was added, whereas the addition of some nitro-free aromatics including fluorophenol, difluoropheol, trifluorophenol, benzonitrile, benzoic acid, aniline, and sodium benzoate did not cause obvious fluorescence changes (Figure S17, Supporting Information), which indicated the good selectivity of the SCD–AnEA fluorescent probe to NACs. In addition, the mixture of 2,4,6-trinitrophenol, sodium benzoate, aniline, and 3,4,5-trifluorophenol was used to simulate real samples, resulting in almost the same fluorescence quenching degree of SCD–AnEA as TNP alone (Figure S18, Supporting Information). These phenomena jointly indicated that the SCD–AnEA assembly has high selectivity and anti-interference ability to the detection of TNP in water.

To quantitatively study the quenching rate and the determination limit, the emission response of SCD–AnEA was investigated by the Stern–Volmer (SV) relationship.[47,48] The SV plot of TNP is a nonlinear curve, which is applicable to the SV equation ($I_0/I = \mathrm{A}e^{K[Q]} + \mathrm{B}$), where I_0 and I are fluorescence intensities before and after addition of TNP, [Q] is the molar concentration, and $K_{S–V}$ is the quenching constant (M^{-1}). The $K_{S–V}$ constant of SCD–AnEA for TNP was calculated to be 1.18×10^5 M^{-1} and the detection limit was 586 ppb in water,[49] demonstrating the high detection sensitivity toward TNP. According to the nonlinear

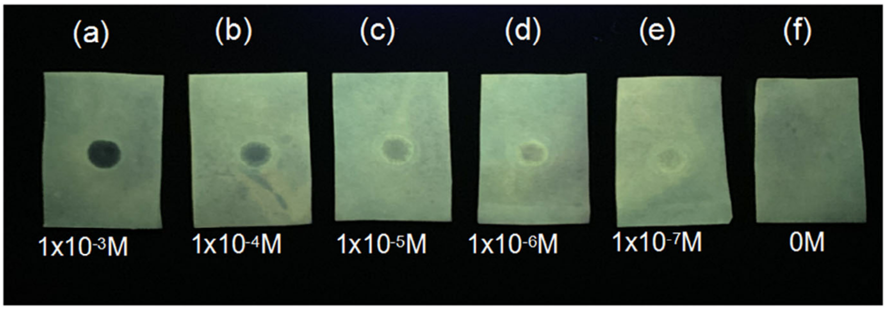

Figure 4. Visual detection of TNP of different concentrations by the paper test strips coated with SCD–AnEA probe (under 365 nm light).

feature of the SV plot (Figure 3c), we deduced that the possible fluorescence quenching mechanism may be that the high-electron-deficient property of the NACs facilitated the efficient photoinduced electron transfer (PET) from the electron-rich SCD–AnEA assembly (donor)[50–52] (**Scheme 2**). The redox potential was measured by cyclic voltammetry using the $Fe(CN)_6^{3-}$/$Fe(CN)_6^{4-}$ solution with the concentration ratio of 1:1 which was used as a blank control. After adding SCD–AnEA (5.71×10^{-6} M/4×10^{-5} M) and TNP (4×10^{-5} M), the peak current between the electrodes was increased, which indicated that electron transfer occurred (Figure S19, Supporting Information). Significantly, the SCD–AnEA probe also exhibited good fluorescence-sensing ability to TNP after being attached to the filter paper (**Figure 4**). Herein, the filter paper was immersed in an aqueous solution of SCD–AnEA (SCD:AnEA = 1:7, AnEA = 4×10^{-5} M) for 4 h and then naturally dried for 12 h in the dark. TNP solutions of different concentrations were prepared, and 5 μL of each solution was dropped on the test paper. As shown in Figure 4, the fluorescence of the filter paper containing SCD–AnEA quenched, showing black spots under illumination of 365 nm. The minimum concentration of TNP that can be detected by the SCD–AnEA test paper was 10^{-7} M, i.e., 23 ppb. However, the test paper showed moderate-to-weak detection effect toward other nitro-compounds (ONP, PNT, DNP, and DNT) under the same condition. In the control experiment, different analyte solutions at 1×10^{-3} M were dropped on the test paper, and TNP presented the most obvious black spot (Figure S20, Supporting Information), which is consistent with the selectivity of SCD–AnEA probe in water.

3. Conclusion

In conclusion, an effective supramolecular fluorescent probe was prepared via the SCD-induced molecular aggregation of AnEA and the subsequent AIE fluorescence emission. The SCD–AnEA probe exhibited good detection universality toward the explosive NACs in water. Significantly, the SCD–AnEA probe presented high sensitivity and anti-interference ability toward TNP with a fluorescence quenching efficiency up to 95% in water as well as a detection limit as 586 ppb in water and 23 ppb on the test paper. This work provides an effective and convenient supramolecular strategy for the preparation of fluorescent sensors and is of great significance in the practical application of detecting nitro-compound contamination in water.

4. Experimental Section

Materials and Methods: All the chemicals were available commercially and used without further purification. 9,10-Bis(diethylphosphonomethyl) anthrance was purchased from Meryer. 4-Hydroxybenzaldehyde was purchased from Ark Pharm. Hexamethylene dibromide was purchased from Adamas. Potassium *tert*-butoxide was purchased from Aladdin. Sulfato-β-cyclodextrin (SCD, sulfated sodium salt extent of labeling: 12–15 mol per mol β-CD) was purchased from Sigma-Aldrich. ^{1}H NMR spectra and ^{13}C NMR spectra were conducted on a Bruker AV100 instrument at 25 °C. Mass spectra were recorded with an IonSpec QFT-ESI MS. UV–vis absorption spectra and the optical transmittance were recorded in a quartz cell (light path: 10 mm) on a Shimadzu UV-3600 spectrophotometer. Fluorescence emission spectra were recorded in a conventional quartz cell (10 × 10 × 45 mm) at 25 °C on a Varian Cary Eclipse equipped with a Varin Cary single-cell peltier accessory to control temperature. All fluorescence emission spectra were conducted with the 5/5 slit unless otherwise indicated. TEM images were obtained on a Philips Tecnai G2 20 S-TWIN high-resolution transmission electron microscope at an accelerating voltage of 200 keV. The samples were prepared by dropping the solution onto a carbon-coated copper grid and air dried. SEM images were characterized on a JEOL JSM-7500F SEM at 30 keV. The samples were examined on a laser light-scattering spectrometer (BI-200SM) equipped with a digital correlator (TurboCorr) at 636 nm at a scattering angle of 90°. Zeta potential values were determined at 25 °C on a Brookhaven ZetaPALS (Brookhaven Instrument, USA). The instrument utilized phase-analysis light scattering to provide an average over multiple particles. Doubly distilled water was used as the background electrolyte for zeta potential measurements. All experiments were conducted in deionized water at 25 °C unless otherwise indicated.

Synthesis of AnEA: Compound 1 was purchased from Meryer and used without further purification. Compound 2 was synthesized based on the previous report.[1] Compound 1 (1 mmol, 478.46 mg) was dissolved in dry THF (42 mL) under nitrogen, and then potassium *tert*-butoxide (3 mmol, 336.63 mg) was added. The mixture was stirred in an ice bath for 1 h. Compound 2 (2.4 mmol, 684.432 mg) was dissolved in dry THF (10 mL) and added to the above solution through a drip funnel. After that, the ice bath was removed, and the solution was stirred at room temperature and for 24 h. The reaction solution was dried via rotary evaporation under reduced pressure. Dichloromethane (2.5 mL) was added to obtain a suspension that was then dropped into methanol (100 mL) to produce a yellow solid. The solvent was removed by filtration, and the yellow solid was washed with methanol three times, and then dried under vacuum to obtain Compound 3 (yield: 503.31 mg, 68%) (Scheme 2).

Compound 3 (0.135 mmol, 100 mg) was dissolved in DMF (5 mL), and trimethylamine ethanol solution (1 mL) was added. The mixture was heated and refluxed at 80 °C for 24 h. Most of the solvent was removed by vacuum distillation, and the crude product was washed by ether three times. Ultimately, the product AnEA was dried overnight under vacuum (yield: 93.87 mg, 80%). ^{1}H NMR (400 MHz, DMSO-d$_6$): δ8.39 (d, 4H), 7.99 (d, 2H), 7.77 (d, 4H), 7.56 (d, 4H), 7.04 (d, 4H), 6.89 (d, 2H),

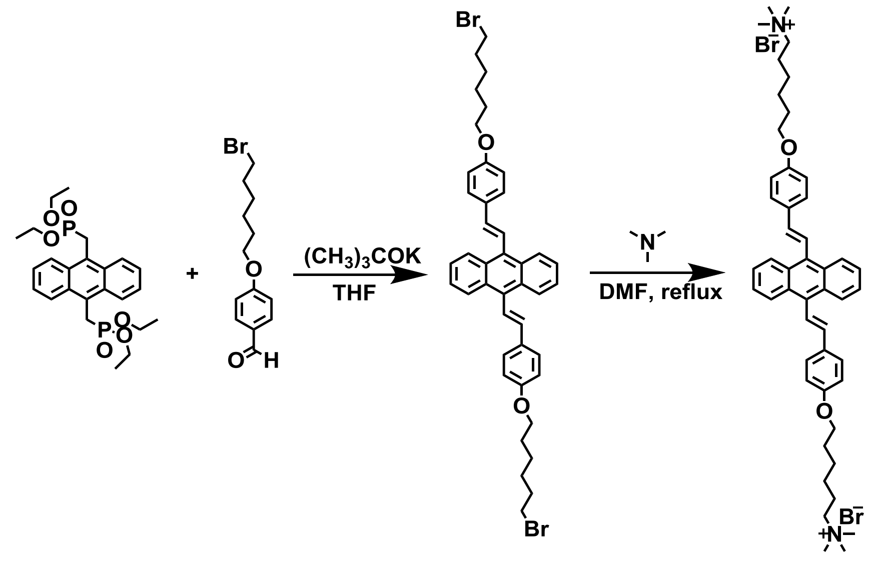

1 2 3 AnEA

Scheme 2. Synthesis of AnEA.

4.06 (t, 4H), 3.28 (t, 4H), 3.06 (s, 18H), 1.81 (m, 4H), 1.56 (m, 4H), 1.41 (m, 4H). ^{13}C NMR (100 MHz, DMSO-d$_6$): δ159.17, 137.22, 132.84, 130.03, 129.46, 128.59, 126.73, 125.94, 122.69, 115.17, 67.87, 65.70, 52.62, 28.90, 26.01, 25.59, 22.49. ESI-MS: *m*/*z* 349.24 ([AnEA-2Br]$^{2+}$/2, calculated for $C_{48}H_{62}N_2O_2{}^{2+}$/2, 349.24).

Preparation of Supramolecular Aggregates: SCD and AnEA were dissolved in Milli-Q water under vigorous sonication. The SCD and AnEA solutions were mixed in a molar ratio of 7:1, and then an appropriate amount of water was added. SCD–AnEA supramolecular aggregates were obtained by the mixed solution.

Fluorescence Emission Spectra: About 150 µL of 8×10^{-4} M AnEA, 17.14 µL of 1×10^{-3} M SCD, and 2832.86 µL of water were fully mixed. Then, the mixture was transferred to the quartz cell. The fluorescence emission spectra and intensity were recorded in the range of 430–800 nm ($\lambda_{ex} = 420$ nm).

Emission Quenching Experiments: The emission quenching experiments were conducted at concentrations of SCD and AnEA of 5.71×10^{-6} M and 4×10^{-5} M, respectively. TNP was added to the SCD–AnEA assembly solution (3 mL) to detect its fluorescence quenching. The analyte solutions were prepared and 5 µL of each solution was dropped on the test paper. The detection in water cost less than 1 min and the test paper detection cost about 3 min until the solvent evaporated to dryness.

Supporting Information

Supporting Information is available from the Wiley Online Library or from the author.

Acknowledgements

This work was financially supported by the National Natural Science Foundation of China (grant nos. 21672113, 21772099, 21861132001, and 21971127).

Conflict of Interest

The authors declare no conflict of interest.

Keywords

nitroaromatic explosives, sulfato-β-cyclodextrin, supramolecular probes, water

Received: July 13, 2020
Revised: August 14, 2020
Published online:

---

[1] L. B. Barber, S. H. Keefe, G. K. Brown, E. T. Furlong, J. L. Gray, D. W. Kolpin, M. T. Meyer, M. W. Sandstrom, S. D. Zaugg, *Environ. Sci. Technol.* **2013**, *47*, 2177.
[2] S. Sood, A. Umar, S. K. Mehta, S. K. Kansal, *J. Colloid Interface Sci.* **2015**, *450*, 213.
[3] A. Chowdhury, P. Howlader, P. S. Mukherje, *Chem. Eur. J.* **2016**, *22*, 7468.
[4] Z. Hu, B. J. Deibert, J. Li, *Chem. Soc. Rev.* **2014**, *43*, 5815.
[5] S. Pramanik, Z. Hu, X. Zhang, C. Zheng, S. Kelly, J. Li, *Chem. Eur. J.* **2013**, *19*, 15964.
[6] S. Sanda, S. Parshamoni, S. Biswas, S. Konar, *Chem. Commun.* **2015**, *51*, 6576.
[7] J. Shen, J. Zhang, Y. Zuo, L. Wang, X. Sun, J. Li, W. Han, R. He, *J. Hazard. Mater.* **2009**, *163*, 1199.
[8] J. D. Rodgers, N. J. Bunce, *Water Res.* **2001**, *35*, 2101.
[9] S. Wasi, S. Tabrez, M. Ahmad, *Environ. Monit. Assess.* **2013**, *185*, 2585.
[10] A. Chowdhury, P. S. Mukherjee, *J. Org. Chem.* **2015**, *80*, 4064.
[11] S. S. Nagarkar, A. V. Desai, P. Samanta, S. K. Ghosh, *Dalton Trans.* **2015**, *44*, 15175.
[12] K. Acharyya, P. S. Mukherjee, *Chem. Commun.* **2014**, *50*, 15788.
[13] P. G. Thorne, T. F. Jenkins, *Field Anal. Chem. Technol.* **1997**, *1*, 165.
[14] P. Ghosh, S. K. Saha, A. Roychowdhury, P. Banerjee, *Eur. J. Inorg. Chem.* **2015**, *2015*, 2851.
[15] S. Cheng, J. Dou, W. Wang, C. Chen, L. Hua, Q. Zhou, K. Hou, J. Li, H. Li, *Anal. Chem.* **2013**, *85*, 319.
[16] E. Wallis, T. M. Griffin, J. N. Popki, M. A. Eagan, R. F. McAtee, D. Vrazel, J. McKinly, *Proc. SPIE Int. Soc. Opt. Eng.* **2005**, *5795*, 54.

[17] K. M. Roscioli, E. Davis, W. F. Siems, A. Mariano, W. Su, S. K. Guharay, H. H. Hill, *Anal. Chem.* **2011**, *83*, 5965.
[18] D. R. Ifa, N. E. Manicke, A. L. Dill, R. G. Cooks, *Science* **2008**, *321*, 805.
[19] R. Mu, H. Shi, Y. Yuan, A. Karnjanapiboonwong, J. G. Burken, Y. Ma, *Anal. Chem.* **2012**, *84*, 3427.
[20] J. M. Sylvia, J. A. Janni, J. D. Klein, K. M. Spencer, *Anal. Chem.* **2000**, *72*, 5834.
[21] E. L. Holthoff, D. N. Stratis-Cullum, M. E. Hankus, *Sensors* **2011**, *11*, 2700.
[22] S. W. Thomas, G. D. Joly, T. M. Swager, *Chem. Rev.* **2007**, *107*, 1339.
[23] S. Rochat, T. M. Swager, *ACS Appl. Mater. Interfaces* **2013**, *5*, 4488.
[24] S. W. Thomas, G. D. Joly, T. M. Swager, *Chem. Rev.* **2007**, *107*, 1339.
[25] S. Rochat, T. M. Swager, *ACS Appl. Mater. Interfaces* **2013**, *5*, 4488.
[26] Y. Yang, H. Wang, K. Su, Y. Long, Z. Peng, N. Li, L. Feng, *J. Mater. Chem.* **2011**, *21*, 11895.
[27] Y. Z. Liao, V. Strong, Y. Wang, X. Li, X. Wang, R. B. Kaner, *Adv. Funct. Mater.* **2012**, *22*, 726.
[28] V. Bhalla, A. Gupta, M. Kumar, S. D. S. Rao, S. K. Prasad, *ACS. Appl. Mater. Interfaces* **2013**, *5*, 672.
[29] S. Barman, J. A. Garg, O. Blacque, K. Venkatesan, H. Berke, *Chem. Commun.* **2012**, *48*, 11127.
[30] K. K. Kartha, S. S. Babu, S. Srinivasan, A. Ajayaghosh, *J. Am. Chem. Soc.* **2012**, *134*, 4834.
[31] M. Kaur, S. K. Mehta, S. K. Kansal, *Spectrochim. Acta A* **2017**, *180*, 37.
[32] A. C. P. Swamy, P. Thilagar, *Chem. Eur. J.* **2015**, *21*, 8874.
[33] M. Ahmeda, S. Hameeda, A. Ihsanb, M. M. Naseer, *Sens. Actuators, B* **2017**, *248*, 57.
[34] Z. Hu, B. J. Deibert, J. Li, *Chem. Soc. Rev.* **2014**, *43*, 5815.
[35] P. Ghosh, S. K. Saha, A. Roychowdhury, P. Banerjee, *Eur. J. Inorg. Chem.* **2015**, *2015*, 2851.
[36] B. Gole, S. Shanmugaraju, A. K. Bar, P. S. Mukherjee, *Chem. Commun.* **2011**, *47*, 10046.
[37] S. Shanmugaraju, H. Jadhav, R. Karthik, P. S. Mukherjee, *RSC Adv.* **2013**, *3*, 4940.
[38] L. Shao, J. Sun, B. Hua, F. H. Huang, *Chem. Commun.* **2018**, *54*, 4866.
[39] J. Yu, Y. Chen, J. J. Li, Y. Liu, *J. Mater. Chem. C* **2017**, *5*, 799.
[40] Z. Wang, B. Xu, L. Zhang, J. B. Zhang, T. Ma, J. H. Zhang, X. Q. Fu, W. J. Tian, *Nanoscale* **2013**, *5*, 2065.
[41] S. Kim, Q. Zheng, G. S. He, D. J. Bharali, H. E. Pudavar, A. Baev, P. N. Prasad, *Adv. Funct. Mater.* **2006**, *16*, 2317.
[42] X. F. Hou, Y. Chen, Y. Liu, *Soft Matter* **2015**, *11*, 2488.
[43] L. Wang, B. Xu, J. Zhang, W. Tian, *Chem. Chem. Phys.* **2013**, *15*, 2449.
[44] Y. X. Wang, Y. M. Zhang, Y. Liu, *J. Am. Chem. Soc.* **2015**, *137*, 4543.
[45] A. Sil, D. Giri, S. K. Patra, *J. Mater. Chem. C* **2017**, *5*, 11100.
[46] Y. Hong, W. J. Y. Lam, B. Z. Tang, *Chem. Commun.* **2009**, *29*, 4332.
[47] X. Zhang, G. Ren, M. Li, W. Yang, Q. Pan, *Cryst. Growth Des.* **2019**, *19*, 6308.
[48] Y. Li, K. Liu, W. J. Li, A. Guo, F. Y. Zhao, H. Liu, W. J. Ruan, *J. Phys. Chem. C* **2015**, *119*, 28544.
[49] D. Dinda, A. Gupta, B. K. Shaw, S. Sadhu, S. K. Saha, *ACS Appl. Mater. Interfaces* **2014**, *6*, 10722.
[50] Y. Dong, B. Xu, J. Zhang, H. G. Lu, S. P. Wen, F. P. Chen, J. T. He, B. Li, L. Ye, W. J. Tian, *Crystengcomm* **2012**, *14*, 6593.
[51] H. T. Feng, Y. S. Zheng, *Chem. Eur. J.* **2014**, *20*, 195.
[52] J. Liu, Y. Zhong, P. Lu, Y. Hong, W. Y. Lam, M. Faisal, Y. Yu, K. S. B. Wong, Z. Tang, *Polym. Chem.* **2010**, *1*, 426.